JOURNAL OF MATERIALS SCIENCE 22 (1987) 798–802

Chill block melt spinning of nickel–molybdenum alloys

KEVIN J. HEMKER, THOMAS K. GLASGOW
Solidification Fundamentals Section, Materials Division, NASA Lewis Research Center, Cleveland, Ohio 44135, USA

Samples of Ni–Mo alloys ranging in composition from pure nickel to Ni–40 at% molybdenum were cast by the chill block melt spinning rapid solidification technique and examined by optical metallography, X-ray diffraction, and microhardness testing. Casting difficulties were encountered with lean alloys, but richer alloys spread more readily on the casting wheel. Alloy microstructures for 5 to 37.5 at% molybdenum ribbons were primarily cellular/dendritic; microstructure feature size decreased with increasing molybdenum content. Extended solubility of molybdenum in γ-nickel, with fcc lattice parameter increasing with composition to the 1.05 power, was observed up to 37.5 at% molybdenum. Substoichiometric Ni–Mo (δ) nucleated on the wheel side of the ribbons of compositions 35, 37.5, and 40 at% molybdenum. The amount of partitionless δ phase thus formed increased with increasing molybdenum content and quench rate. This substoichiometric δ transformed readily to a fine structured γ–δ mixture.

1. Introduction

Rapidly solidified alloys typically exhibit unusual microstructures, decreased segregation, very fine grain size, and potentially, improved properties. This study of the binary nickel–molybdenum (Ni–Mo) eutectic system was undertaken as an aid to the investigation of other more complex nickel–base alloy systems and was limited to metallographic, X-ray, and microhardness analysis. It was undertaken with the following preliminary areas of interest: to make a general observation of eutectic behaviour during rapid solidification, to determine the amount of any increase in solid solubility, to identify the formation of any metastable phases, and to determine the effect of composition on melt-spinning castability.

The equilibrium phase diagram from Shunk [1] for the Ni–Mo eutectic system is shown in Fig. 1. At equilibrium the maximum solubility of molybdenum in the fcc nickel phase (γ) is 28.4 at % at the eutectic temperature, 1318° C. Ni–Mo (δ), as a single phase, is found at equilibrium only for compositions in the range of 51 to 53 at % molybdenum. Between 28.4 and 51 at % molybdenum proportionate amounts of both γ and δ are formed under equilibrium conditions.

2. Experimental procedure

The Ni–Mo ribbons used in this study were cast by the free jet chill block melt spinning (CBMS) process at NASA's Lewis Research Center. For a full explanation of the casting apparatus see [2]. Casting was performed in both vacuum and helium atmospheres. The charge of 12 to 20 g was heated to approximately 50° C above the liquidus temperature and discharged onto a 4340 steel wheel finished with 600 grit paper. The ejection pressure used was 86 kN m^{-2}, the ejection orifice was 1 mm in diameter, and the wheel surface speed was 20 m sec^{-1}.

The alloy compositions cast were: Ni–0, 5, 17.5, 21, 28, 35, 37.5 and 40 at % Mo. They are shown in Fig. 1 in relation to the equilibrium phase diagram; the elevation of each "x" indicates the casting temperature.

All ribbons cast were examined by X-ray diffraction on both free and wheel sides for phase identification and measurement of the fcc phase lattice parameter. Samples mounted on edge were polished and etched with Marbles etchant for metallographic examination. Knoop microhardness measurements were taken on all samples using a 10 g load.

In addition, three compositions, Ni–19, 25, and 35 at % Mo, were melted and allowed to cool to room temperature in their crucibles. These samples are referred to as "conventionally cast samples", and were characterized by X-ray diffraction for comparison with the rapidly solidified ribbons.

3. Results

3.1. General observations

Ribbons cast for this work were approximately 40 μm thick, 2.5 mm wide, and in lengths as long as 15 m. The castability of pure nickel was poor and no single layer ribbons were obtained. Ribbon lengths and castability increased with increasing molybdenum content. This observation seems to be general. Several transition metal based alloys have been cast at NASA Lewis. In each case difficulty has been encountered with the pure metal or lean alloy while richer alloys, including eutectics, cast well. Ribbons with 40 at % molybdenum cast well, but were brittle and shattered upon impact with the chamber walls after leaving the wheel.

3.2. X-ray

X-ray analysis yielded the following results. The nickel fcc phase (γ) was identified in all ribbons. The

0022–2461/87 $03.00 + .12

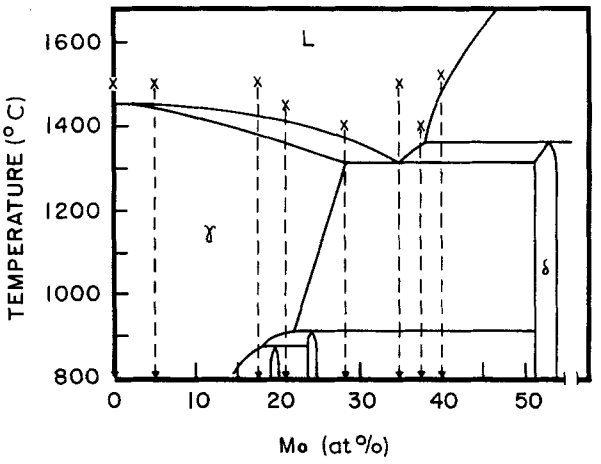

Figure 1 Nickel–molybdenum phase diagram; (x) indicates both pre-casting hold temperatures and compositions cast.

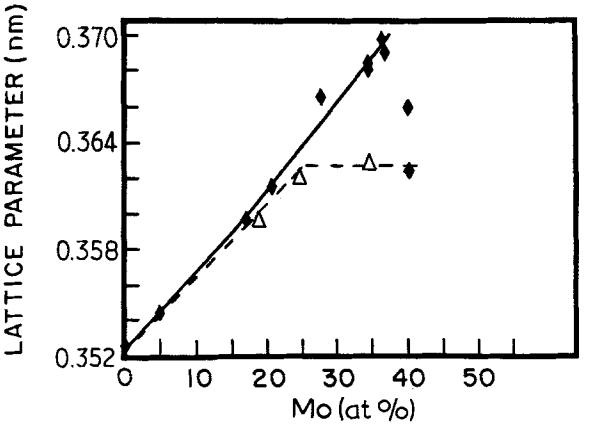

Figure 2 Lattice parameters of the fcc nickel-based γ phase as a function of composition for (△) conventionally cast and (◆) rapidly solidified Ni–Mo alloys.

lattice parameter of this phase increased with increasing molybdenum content to 37.5 at % molybdenum. At 40 at % molybdenum the fcc lattice parameter measured decreased to a value much closer to equilibrium value. The lattice parameter, a_0, of the γ phase as a function of composition is shown in Fig. 2, and can best be represented by the equation:

$$a_0 = 3.524 + 0.0035 \text{ (at \% Mo)}^{1.05}$$

Though not shown in Fig. 2, literature values for 0 to 20 at % molybdenum, quenched in the solid state [3, 4], fall on the same curve. fcc (γ) and Ni–Mo (δ) were both identified on both sides of the 40 at % molybdenum ribbon. Unit cell size for the orthorhombic δ was variable and slightly smaller than reference values for δ. Indications of δ were found only on the wheel side for ribbons of 35 and 37.5 at % molybdenum. Unit cell size for these could not be determined. Several additional lines were observed but could not be indexed.

3.3. Metallography

Metallographic analysis of multiple layer pure nickel ribbon showed very large grains. Alloys of 5 to 28 at % molybdenum, those conventionally in the γ solid solution range, showed cellular/dendritic growth. The cell/dendrite width decreased with increasing molybdenum content, Fig. 3. Three zones were observed in the 35 at % molybdenum ribbon, Fig. 4. A thin zone, featureless at × 1000, appeared closest to the wheel. Directly adjacent and separated by a grain boundary was a planar front growth zone. Grains of the planar front zone evidently choked off the featureless zone. As the planar front zone broke down, cellular/dendritic grains formed. This third, cellular/dendritic zone occupied about two thirds of the ribbon thickness. A shaded band ran lengthwise along the approximate middle of the ribbon. These features were repeated in the 37.5 at % molybdenum ribbon, but the featureless zone was thicker for the 37.5 at % molybdenum ribbon than for the 35 at % ribbon, Fig. 4. Cracks were evident in the featureless zone for the 37.5 at % ribbon. The 40 at % molybdenum ribbon showed two distinct areas, Fig. 5. In most of the 40 at % molybdenum sample a very fine dark etching structure was observed. In some areas this fine structure abutted a featureless zone that extended through the entire thickness of the foil.

Casting in a helium atmosphere rather than vacuum served to increase the thickness of the featureless zone for both the 35 and 37.5 at % molybdenum samples. In the 37.5 at % molybdenum ribbon cast in helium, a

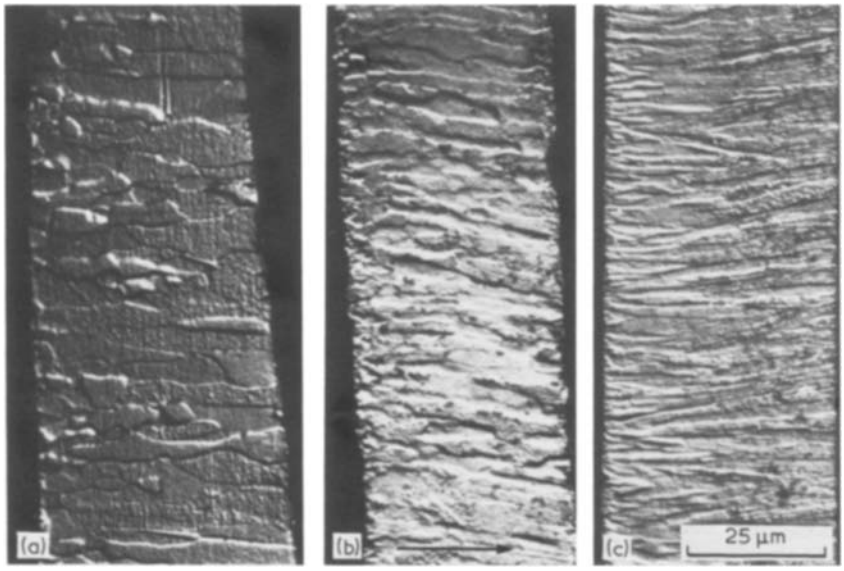

Figure 3 Cellular dendritic structure for chill-block melt-spun ribbons with (a) 5 at % Mo; (b) 17.5 at % Mo; and (c) 28 at % Mo. Arrow, growth direction.

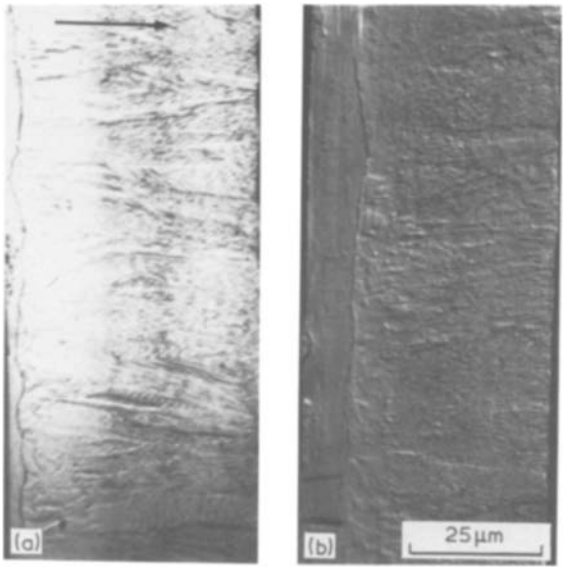

Figure 4 Eutectic and hypereutectic ribbons showing the "featureless" substoichiometric δ NiMo zone, and intervening planar front zone, and the cellular dendritic structure; (a) 35 at % Mo; and (b) 37.5 at % Mo. Arrow, growth direction.

range of microstructures indicating transformation of the featureless zone to a fine structure was observed, Fig. 6. Isothermal anneals of 37.5 at % molybdenum ribbon confirmed that the dark etching, fine structure, formed by a solid state transformation; this rapid transformation occurred at temperatures above 800° C.

3.4. Microhardness

Microhardness readings were taken for each of the three major structures observed: cellular/dendritic, featureless, and fine structured. Hardness of the cellular/dendritic phase increased with increasing molybdenum content, Fig. 7. Hardness of the featureless phase was much higher than for the cellular/dendritic, and was essentially the same for the three compositions (35, 37.5, and 40 at % molybdenum) at which it was observed. Hardness of this featureless zone was equivalent to a reference Ni–Mo (δ) phase found in an undercooled Ni–Mo eutectic alloy specimen [5]. Hardness of the fine structured region was comparable to the cellular/dendritic phase.

Figure 5 40 at % Mo ribbon showing both featureless substoichiometric δ NiMo and regions of transformed microcrystalline structure. Arrow, growth direction.

4. Discussion

4.1. Extended solubility

The fact that the f c c (γ) lattice parameters determined in this study are in very good agreement with reference values to 20 at % and can be shown as an extension of this data up to 37.5 at % is a clear indication of the extended solid solubility of molybdenum in γ. The solid solubility was extended by rapid solidification from the equilibrium value of 28.4 to 37.5 at % molybdenum.

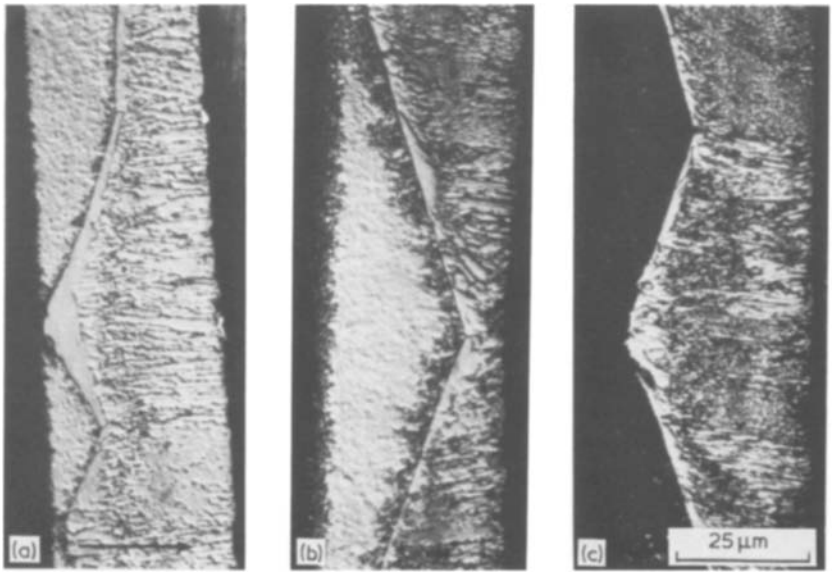

Figure 6 Progression of the transformation from featureless to microcrystalline for 37.5 at % Mo ribbon cast in helium. Transformed material etches darkly: (a) Slightly to (c) completely transformed. Arrow, growth direction.

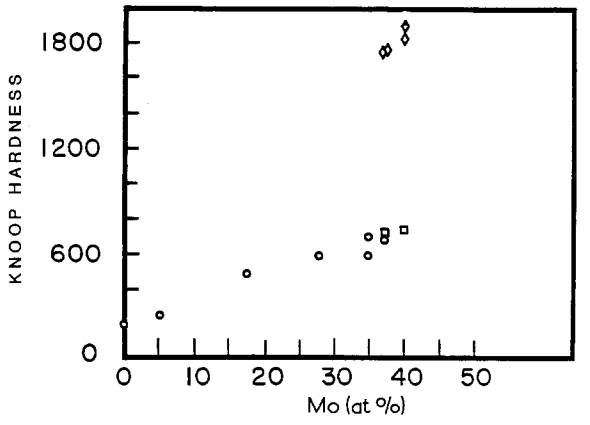

Figure 7 Microhardness of phases present in rapidly solidified Ni–Mo alloys. (○) cellular dendritic γ, (□) fine structured $\gamma + \delta$, (◇) featureless δ.

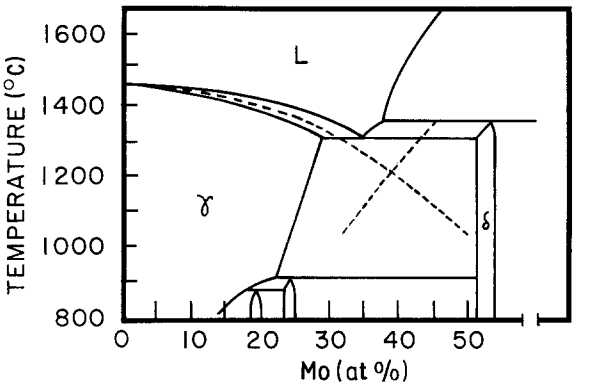

Figure 8 Ni–Mo equilibrium phase diagram showing T_0 lines for γ and δ phases.

The lattice parameters determined for the 40 at % molybdenum ribbons indicate the termination of this extension of the solid solubility of the γ phase.

4.2. Metastable phase formation

Both metallographic observation and hardness measurements confirm that the featureless structures observed in the 35, 37.5, and 40 at % molybdenum ribbons are the same phase. The featureless zone nucleated on the wheel side of the ribbon and grew in thickness with increasing molybdenum content until at 40 at % molybdenum the entire ribbon was featureless. Metallography of the 37.5 at % molybdenum ribbon showed that this featureless zone is a metastable phase which transforms to a microcrystalline structure containing both γ and δ. The transformed product was the dominant microstructure observed in 40 at % molybdenum ribbon. Different portions of the ribbon cool in the solid state at quite different speeds after separation from the casting wheel. This led to varying portions of the retained metastable phase.

The featureless zone present on the wheel side of 35 and 37.5 at % molybdenum ribbons and throughout the 40 at % molybdenum ribbons can be interpreted as a metastable, substoichiometric extension of the Ni–Mo (δ) phase. Hardness and etching response of this featureless zone and a reference Ni–Mo (δ) sample are essentially equal. X-ray results indicate the presence of the δ phase on the wheel side of the 35 and 37.5 at % ribbons and on both sides of the 40 at % molybdenum ribbon. It should be noted that there is no obvious solidification structure evident in the substoichiometric δ phase; it is conceivable that the δ phase forms from a glassy intermediate phase.

It is interesting that the extension of molybdenum solid solubility in γ was limited by the nucleation and growth of a separate phase (greatly substoichiometric δ), not by equilibrium precipitation of the eutectic mixture of γ and δ. The initial nucleation of substoichiometric δ and the subsequent nucleation and dominant growth of extended solid solution γ seen in 35 and 37.5 at % molybdenum alloys is important. It indicates that metastable δ is an easily nucleated but slow growing phase; moreover, that supersaturated γ is relatively difficult to nucleate but grows rapidly. This conclusion is supported by observations in other studies. In a Ni–35 at % Mo alloy undercooled in a glass slag atmosphere it has been observed that δ is a poor heterogeneous nucleant for the γ phase; and dendrites of faceted δ phase grow at a much lower rate compared to the γ dendrites for the same amount of melt undercooling [6]. The sensitivity of the Ni–Mo system to change in cooling condition at 35 and 37.5 at % molybdenum suggests its utility in comparing rapid solidification techniques.

The precipitation of greatly substoichiometric δ implies very substantial undercooling at the solidification front, e.g., about 225° C below the equilibrium liquidus for the 40 at % molybdenum composition. At this composition and under slow cooling conditions, primary molybdenum could form at 1475° C and δ at 1362° C. A temperature, T_0, may be defined at which an undercooled liquid has free energy equal to a solid of the same composition [7]. Below the T_0 temperature partitionless solidification of a crystalline solid is possible. Based on simple linear extrapolation of a T_0 line bisecting the equilibrium δ liquidus and solidus positions, as shown in Fig. 8, partitionless solidification of δ at 40 at % molybdenum would not be expected above about 1250° C. Partitionless formation of δ at 37.5 and 35 at % molybdenum would require even lower temperatures, about 1200 and 1150° C respectively. The competitive replacement of substoichiometric δ with partitionless γ during solidification of 37.5 and 35 at % molybdenum alloys is in accord with an extrapolated T_0 line for the γ phase indicating that γ could form at higher temperatures, i.e., lower undercoolings than δ.

Additional phases were present but could not be identified by X-ray, SEM, or optical metallographic techniques. Transmission electron microscopy studies would greatly improve the understanding of this system and are under way.

4.3. Castability

In conventional casting, mould filling is limited for compositions with a wide spread between liquidus and solidus temperatures. Pure metals or eutectic alloys are thus preferred, and intermediate compositions, having wide mushy zones, are avoided. The observation that ease of melt-spin casting increases with increasing solute content implies that the formation of

a mushy zone aids melt-spin castability. This enhancement extends all the way to the eutectic composition, and in some cases beyond, in accordance with metastable extension of the equilibrium diagram. Comparison with other alloy systems under study [8] indicates that the lower thermal conductivity of alloys compared with pure elements is not a factor, and that numerous systems show greater ease of melt spin casting for rich alloys than for the pure components or for lean alloys.

5. Conclusions

1. Molybdenum solid solubility in γ was extended from 28.4 to 37.5 at % molybdenum by rapid solidification processing.

2. Substoichiometric Ni–Mo (δ) nucleated initially in preference to γ phase for alloys above 35 at % molybdenum. It solidified in a partitionless manner and transformed to a fine structure during cooling.

3. Extension of γ solid solubility is limited by the nucleation of a substoichiometric δ single phase, not by growth of the equilibrium eutectic mixture of γ and δ.

4. Substantial undercoolings, by more than 100° C, at the solidification interface are implied by the occurrence of partitionless δ and γ phases.

5. Finally, it was noted that ease of melt spinning to single layer ribbon increased with increasing solute concentration.

Acknowledgements

The authors wish to thank the following for their contributions to this study: T. J. Moore, N. W. Orth, and R. W. Jech who were responsible for production of the melt-spun ribbons, and R. G. Garlick who contributed greatly with collection and interpretation of X-ray diffraction results.

References

1. F. A. SHUNK, "Constitution of Binary Alloys", Second Supplement (McGraw-Hill, New York, 1969) p. 516.
2. R. W. JECH, T. J. MOORE, T. K. GLASGOW and N. W. ORTH, *J. Metals* **36** (1984) 41.
3. W. B. PEARSON, "Handbook of Lattice Spacings and Structures of Metals and Alloys" (Pergamon Press, Oxford, 1958) p. 753.
4. C. R. BROOKS, J. E. SPRUIELL and E. E. STANSBURY, *Int. Metals Rev.* **29** (1984) 210.
5. S. N. TEWARI, personal communication, August 1984.
6. S. N. TEWARI and T. K. GLASGOW, "Undercooled and Rapidly Quenched Ni–Mo Alloys", NASA TM 87257 (March 1986).
7. J. W. CAHN, in Proceedings of the 2nd International Conference on Rapid Solidification Processing, Reston, Virginia, March 1980, edited by R. Mechrabian, B. H. Kear, and M. Cohen (Claitor's Publishing Division, Baton Rouge, 1980) p. 24.
8. T. K. GLASGOW and R. W. JECH, personal communication, April 1985.

Received 29 October 1985
and accepted 30 June 1986